Journal of Photonic Materials and Technology
2016; 2(3): 25-31
http://www.sciencepublishinggroup.com/j/jpmt
doi: 10.11648/j.jmpt.20160203.12
ISSN: 2469-8423 (Print); ISSN: 2469-8431 (Online)

Thin Films to Single Crystals: Organometal Halide Perovskite Materials for Advanced Optoelectronics

Padmaja Guggilla[1], Ashwith Chilvery[2], Kamala Bhat[1], Edelmy J. Bernardez[2]

[1]Department of Physics, Chemistry, and Mathematics, Alabama A&M University, Normal, USA

[2]Department of Physics and Dual Degree Engineering, Xavier University of Louisiana, New Orleans, USA

Email address:

padmaja.guggilla@aamu.edu (P. Guggilla)

To cite this article:

Padmaja Guggilla, Ashwith Chilvery, Kamala Bhat, Edelmy J. Bernardez. Thin Films to Single Crystals: Organometal Halide Perovskite Materials for Advanced Optoelectronics. *Journal of Photonic Materials and Technology*. Vol. 2, No. 3, 2016, pp. 25-31.
doi: 10.11648/j.jmpt.20160203.12

Received: October 24, 2016; **Accepted**: November 12, 2016; **Published**: December 12, 2016

Abstract: The recent emergence of perovskite materials has revolutionized the photovoltaic (PV) technology and offers solutions to contemporary energy and environmental issues. Moreover, the capabilities of single crystals are far superior to the thin film counterparts. This mini review outlines the growth parameters and crystal kinetics involved in the perovskite single crystal growth process for a superior wafer-style solar cell devices. Typically, perovskite solar cells with perovskite in the film form are attractive with their higher performance but, they degrade at faster rate, suffer immensely from a high density of traps and grain boundaries, which markedly limit the potential performance in devices. This review discusses a list of factors affecting it and provide future prospects of this thriving technology.

Keywords: Perovskites, Single Crystal, Growth Kinetics, Photovoltaics

1. Introduction

Today, the PV technology based on organometallic hybrid perovskites has become a buzzword amongst the scientific community, commercial PV manufacturers, and energy conservationists, due to their superior efficiency, ease of fabrication, low fabrication costs, and scalability. Perovskite solar cells (PSC) are promising with low-cost and pave the roadmap for flexible and highly efficient next-generation solar cells [1–5]. Its unique stoichiometry, hybrid (organic-inorganic framework) structure, and tunable electrical and optoelectronic properties brands them as the best-known devices to transform PV technology. Solar cells composed of organic-inorganic perovskites offer efficiencies approaching that of silicon, but they have been plagued with some important deficiencies limiting their commercial viability.

The hybrid design of organic-inorganic compounds based on methyl ammonium lead halides resembles the perovskite stoichiometry, and inherits many qualities of photovoltaics (PV,) such as stronger and broader absorption, ultra-fast charge transportation, high dielectric, and swift charge recombination [6]. The ease of fabrication, stability, cost, efficiency, and performance of PSCs, rivals the best thin-film PVs; hence, they are the best-chosen material employed to transform PV technology. Half a decade of solar cell research on perovskite materials has enhanced their power conversion efficiencies around 22% [7–9], which makes them the only PV technology to display outstanding potential in the least span of time. The 3D framework of organometal halide (OMH) perovskite materials like methylammonium lead iodide ($CH_3NH_3PbI_3$) supports a multitude of PV functionalities such as light sensitizers, absorbers, and ambipolar electron-hole transporters [10–12]. Additionally, $CH_3NH_3PbI_3$ perovskite has a plethora of electrical properties such as a direct, low bandgap [13] with superior carrier mobility [14], significant ferroelectric [15], and dielectric properties [16].

Despite being a very promising candidate for the solar cell industry, PSCs are currently facing several challenges such as sensitivity to humidity, fast degradation, lead toxicity, and the presence of hysteresis in J-V characteristics [17-19]. A study suggests that dry air is the most suitable storage condition for the device with spiro-OMeTAD hole transport layer and also to achieve high PCEs [20]. Furthermore, the PSCs require flexible encapsulations to retain their PV

performance and allow for a smooth insertion into commercial markets [21-25].

The presence of anomalous J-V hysteresis makes it difficult to reliably quantify the device performance, which could postpone the timely commercialization of this technology. The presence of hysteresis in PSCs is currently speculated to originate from various factors such as scan rate, delay time, sweep direction, interstitial defects, types of charge transport layers, and crystal size, and thickness of the perovskite layer [4, 26, 27]. It was found that the presence of large crystal grain sizes in the perovskite layer and the use of mp-TiO_2 layer can significantly reduce the J-V hysteresis.

Traditionally, the thin film fabrication methodologies have driven the performance and efficiency of perovskite solar cells, and are vital in depositing the light sensitizer OMH perovskite material to enhance the kinetics of the solar cell device. Despite their higher performance, the perovskite devices degrade at a faster rate, which is usually accompanied with color bleaching due to the chemical instability of perovskites in the iodide electrolyte [25]. Recently, researchers have also indicated that single crystalline perovskite materials have potential to further boost photovoltaic device power conversion efficiency to 25% [29]. The overwhelming majority of perovskite devices are based upon polycrystalline thin films–a material that suffers immensely from a high density of traps and grain boundaries, which markedly limit the potential performance in devices. Therefore, a more competitive encapsulation of these properties in a single crystal structure for wafer-style thin films of PV devices can drive farther into commercial markets.

2. Crystal Study of Organometal Halide Perovskites

Typically, the ABX_3 perovskite compound has a crystal structure with a larger metal cation (A), a smaller metal cation (B), and an anion (X) that binds them. In an ideal cubic perovskite structure, the large A cation is in twelve (12) coordination and slightly smaller B cations occupy the octahedral holes formed by the large X anions.

In an idealized cubic perovskite constructed of rigid spheres, each cation is the perfect size to be in contact with an anion, and the radii of the ions are related as

$$R_A + R_X = \sqrt{2}(R_B + R_X) \quad (1)$$

where R_A, R_B, and R_X are the relative ionic radii of the A and B cations, and the X anion, respectively. However, with decreasing A cation size, a point is reached where the cations will be too small to remain in contact with the anions in the cubic structure. This phenomenon of tilting the BX_6 octahedral structure to bring the anions into contact with A cations results in the introduction of a distortion factor, also known as Goldschmidt's tolerance factor [30].

$$R_A + R_X = t\sqrt{2}(R_B + R_X) \quad (2)$$

A tolerance factor (t) close to unity can be considered as an ideal cube [31]. Table 1 displays the possible perovskite structures based on the tolerance factors. Therefore, a precisely engineered material with a perfect crystal structure, such as organometallic halides (OMH), is required for PSCs to act as photosensitizing absorbers.

Table 1. *Possible perovskite structures based on the tolerance factors.*

Structure	Tolerance Factor (t)	Comments	Example
Hexagonal	$t > 1$	$R_A >> R_B$	$BaNiO_3$
Cubic	$0.9 < t < 1$	R_A and R_B can be dissimilar	$SrTiO_3$
Orthorhombic/ Rhombohedral	$0.75 < t < 0.9$	$R_A << R_B$	$CaTiO_3$
Trigonal	$t < 0.7$	$R_A = R_B = R_X$	$FeTiO_3$

The perovskite-structured methylammonium halides (MAH) were first discovered by S. B. Hendricks in 1928 [32], and later studied by several other researchers [33, 34]. However, these materials have displayed unique physical and optoelectronic properties due to the hybrid merging of organic and inorganic materials. The advantages of inorganic components are thermal stability and very high degree of structural order. Organic materials contribute functional versatility, mechanical flexibility, and low cost processing. Combined, they overcome many of the problems associated with creating efficient charge conduction in photovoltaic cells [35]. In the early 1990s, David Mitzi at the IBM Watson Research Centre explored the structural dynamics of methylammonium lead halide ($CH_3NH_3PbI_3$) perovskite materials engineered for niche applications such as electronics, thin film transistors, and light emitting diodes [14, 36–39]. For photovoltaic applications, the large cation A in the OMH crystals is replaced by methylammonium ion ($CH_3NH_3I^+$) (R_A = 1.87 Å), the smaller cation B with Pb^{2+} (R_B = 1.19 Å), and the anion X with halides such as Cl^-(R_X = 1.67 Å), Br^- (R_X = 1.82 Å), I^- (R_X = 2.06 Å). Thus, the above geometry provides a range of tolerance factor ($0.84 < t < 0.86$). The poor anionic features of Fluorine (F), when compared with other halides such as Cl, Br, and I confirm its incompatibility with the symmetry of perovskite structure. Many have also investigated for lead-free OMHs [40, 41], such as Sn^{2+} (R_B = 0.93 Å) with tolerance factor range of ($0.92 < t < 0.95$). It is also possible to tune the electronic, opto-electronic, magnetic and dielectric properties by modifying the stoichiometries of the organic and inorganic components. Thus, the concept of tolerance factor can be understood as a guide to the cubic structures of perovskites. Recently, a comprehensive study on the tolerance factors for over 2300 hypothetical amine–metal–anion permutations based on halides and molecular (organic) anions has revealed that 742 compounds display tolerance factors ranging from 0.8 to 1 [42]. However, the study also reports that of the 742, only 140 of these compounds are known, suggesting further

theoretical and experimental investigation of the remaining 612 for superior PV efficiencies. Figure 1 lists a variety of A, B, and X compounds fitting the cubic perovskite structure based on tolerance factors.

Since hybrid perovskites materials are intrinsically complex, understanding the relationship between structure and optoelectronic properties is very important in terms of presence of various types of interactions and structural disorder that may play an important role in the material properties. Due to the significant role of structural interactions of the organic/inorganic components, different crystallization/deposition methodologies can lead to different crystals with identical nominal chemical composition but with different macroscopic optoelectronic properties [43]. Thus, this futuristic blends of organic and inorganic material can function as a direct absorber of photons, low band-gap semiconductors with good carrier mobility [44].

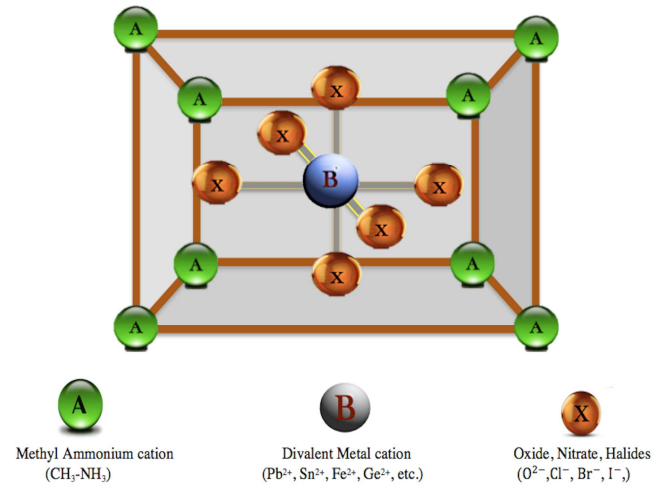

Figure 1. *A list of organic, inorganic, and halide components for A, B, and X stoichiometry of perovskites. Adapted from [6].*

3. Engineering of Crystal Kinetics and Growth Mechanisms

Full structural determination of $MAPbI_3$ single crystals, in particularly the orientational order of MA^+ cation, has been the focus of several experimental 945, 46] and theoretical works [47-49]. Weller et al. characterized the structures of $MAPbI_3$ with neutron powder diffraction and found that the MA^+ cation at room temperature exhibits a high level of orientational motion, adopting four possible orientations along (100) [46]. Several theoretical investigations with ab initio molecular dynamics suggested that the presence of a strong hydrogen bond network keeps the organic cations oriented along specific directions in the tetragonal phase [50].

In our preliminary investigations of solvothermal method, we obtained a methyl ammonium lead bromide single crystal by adding 2.5 g of methylammonium bromide to 8.2g of lead bromide in 20 ml of 48% of hydrobromic acid in water, subsequently fine orange red crystals were obtained over a span of 2-3 hours. To these crystals an additional 20ml of HBr solution is added and the solution was warmed to get a saturated solution. The solution is let aside for crystallization at room temperature. The solid crystals are separated by decantation and the mother liquer was dried overnight in an oven at 70°C. Furthermore, the oven temperature is gradually decreased to room temperature for larger crystals. The crystals obtained were functional and exhibited similar properties as mentioned by other researchers. Powder X-ray diffraction patterns of the ground crystals demonstrate pure perovskite phase for both $MAPbBr_3$ and $MAPbI_3$.

As shown in figure 2, the single crystal X-ray diffraction analysis also showed a good match with previous single crystals grown at room temperature. Further, we investigated optical and transport properties of the crystals, demonstrating that the crystals obtained are comparable quality to previously reported crystals. From the steady-state absorption measurements as shown in figure 3, a band gap extracted from Tauc plots shows values of 2.1 eV for $MAPbBr_3$ and are in good agreement with single crystals grown by other methods [51, 52].

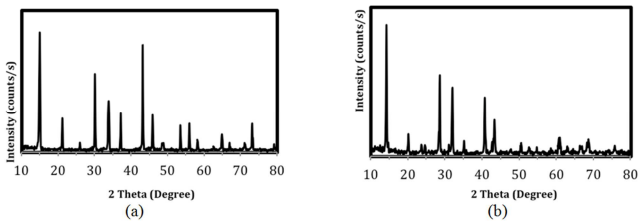

Figure 2. *Powder X-ray diffraction of ground (a) $MAPbBr_3$ and (b) $MAPbI_3$ single crystal.*

These investigations on a single functional crystal of methyl ammonium lead iodide ($CH_3NH_3PbI_3$) indicates that on further optimization in temperature-controlled environments; crystals with superior functionalities, uniform shape and size can be achieved. However, a quantum of research challenges pertaining to these crystals such as transient traps, dynamic and structural orientations, charge carrier and its conduction, and dielectric mapping are yet to be studied.

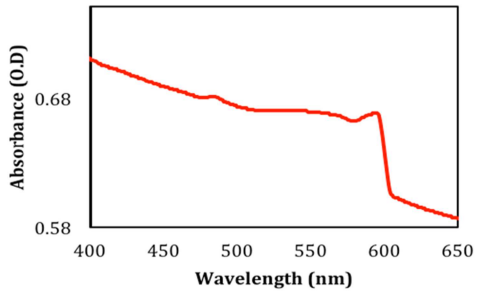

Figure 3. *UV-Vis spectra of $MAPbBr_3$ single crystal.*

The hybrid OMH perovskites are intrinsically complex materials, where the presence of various types of interactions, defects and structural disorder may play an important role in the material properties. Thus, it is required to investigate a relationship between the structure and its impact on optoelectronic properties. Bastiani et al, reported an *in situ*

method for the crystallization of perovskite thin films on different natured substrates such as porous, wet and etc. Through photoluminescence (PL) studies, they demonstrated that the nature of the substrate critically affects the structural and optical properties of the perovskite films by changing the crystallization dynamics [53].

In early 2015, Nie et al, reported on a solution-based hot-casting technique to grow continuous, pinhole-free thin films of OMH perovskites with millimeter-scale (1-2mm) crystalline grains, where hysteresis-free devices were achieved with a power conversion efficiency of 18% for planar solar cell devices [54]. The hot-casting technique incorporated experiences excess solvent volume when the substrate is maintained above the crystallization temperature for the formation of the perovskite phase. This allows for the prolonged growth of the perovskite crystals, yielding large crystalline grains. Furthermore, this technique also attributes for improved PV performance by reducing the bulk defects and improving charge carrier mobility in large-grain devices and paves the way towards the synthesis of wafer-scale crystalline perovskites, for the fabrication of high-efficiency solar cells.

Simultaneously, other researchers have demonstrated that synthesis of large single crystals of OMH perovskites is key to optimize the three figures of merit: charge carrier lifetime, mobility, and diffusion lengths. Shi et al, reported on anti-solvent vacuum assisted crystallization method using a solvent with high solubility for sizable crack-free $MAPbX_3$ single crystals with volumes exceeding 100 cubic millimeters [55]. A comprehensive analysis of carrier lifetime (τ), transient absorption and photoluminescence spectra these crystals exhibited a superposition of fast and slow dynamics: $\tau \approx 41$ and 357 ns for $MAPbBr_3$, and $\tau \approx 22$ and 1032 ns for $MAPbI_3$. It was also observed that the defect density measured for the room temperature–grown $MAPbX_3$ crystals was superior to a wide array of established and emerging optoelectronic inorganic semiconductors including polycrystalline Silicon.

Millimeter sized $CH_3NH_3PbI_3$ single crystals using the low temperature solution approach demonstrated by Dong et al., showed that both the electrons and holes were found to have variable diffusion lengths of >175mm under 1 sun illumination and >3mm under weak illumination of 0.003% sun [56]. Large-sized $CH_3NH_3PbI_3$ single crystals were grown from a supersaturated $CH_3NH_3PbI_3$ solution using a top-seeded solution growth method with a temperature gradient and using the small-sized $CH_3NH_3PbI_3$ single crystals at the bottom of the container maintaining MA^+, Pb^{2+}, and I^- ion concentration for a saturated solution. In this procedure the cooler top half of the solution was super-saturated. Hence it is proved that the large $CH_3NH_3PbI_3$ single crystals can be grown by the consumption of small $CH_3NH_3PbI_3$ single crystals in the bottom. The small temperature difference between the bottom and the top of the solution induces the sufficient convection to transport the material to the large $CH_3NH_3PbI_3$ single crystals. The $CH_3NH_3PbI_3$ single crystals grown in this method had an average size of 3.3 mm and a largest size of ~10 mm.

Furthermore, $CH_3NH_3PbI_3$ solar cell configuration can be produced by depositing the material using the spin coating technique on TiO_2 nanoparticles and using a solid state redox mediator reported light conversion efficiency (η) up to 16%, an unprecedented value for such a device [57]. Some of the advantages of this material are the high cross section for photo-electron generation, the long diffusion length of the charge carriers and the simplicity of $CH_3NH_3PbI_3$ synthesis and device architecture. This method also reported the decrease in the value of η due to the lack of its evacuation, which resulted in mechanical stress in the sandwich-structured device and over time that cause structural decoupling of the constituents.

Though $CH_3NH_3PbI_3$ has been reported as an excellent perovskites crystal structure for using as an efficient solar cell; the global concern about the toxicity of Pb mandates the scientists to look for alternatives [58]. Favorable bandgap, high optical absorption coefficient, and low exciton binding energies indicate that $CsSnI_3$ is a viable candidate as a light absorber for lead free perovskite solar cells. $CsSnI_3$ layers were spin coated on to ~300 nm thick mesoporous layers. Kumar et al., reported that usage of dimethyl formamide (DMF) and 2-methox-yethanol as solvents for the $CsSnI_3$ resulted in the formation of large islands on the TiO_2 scaffold, with significant areas of exposed TiO_2 and more complete coverage and good pore filling of $CsSnI_3$ [50, 59].

Hao et. Al reported that the lead-free perovskite of methylammonium tin iodide ($CH_3NH_3SnI_3$) as the light-absorbing material to fabricate solution-processed solid-state photovoltaic devices which has the much lower optical bandgap of 1.3 eV than the $CH_3NH_3PbI_3$ (1.55 eV). Fabrication of these photovoltaic devices was done by spin coating a solution of colloidal particles (20 nm) onto a 30-nm-thick compact TiO_2 in a nitrogen glove box thus avoiding hydrolysis and oxidation of the tin perovskite by contact with air [60]. It is also reported that the under layer was deposited by atomic layer deposition on a pre-patterned transparent-conducting-oxide-coated glass. Optical properties of perovskite films are dependent on the grain size of the material that mandates the full characterization of the sample from which the optical constants are extracted. Since large $CH_3NH_3PbBr_3$ crystals properties would vary from the kinetically control processed films, Brittman and Garnett suggested a direct comparison of micro scale reflectance and transmittance measurements on films as well as single crystals of $CH_3NH_3PbBr_3$ produced by stamping with polydimethylsiloxane [61]. Reports indicate that in $CH_3NH_3PbBr_3$ crystals the properties are considerably enhanced compared to their polycrystalline thin film counterparts due to the absence of an absorption peak near the band gap of the crystals [62, 63].

Giacomo and Maculan reported that $CH_3NH_3PbCl_3$ based UV-photo detector also reported to provide high detectivity and ON-OFF ratio, with a response time in the order of milliseconds thus making them useful in optoelectronic devices [59]. Since the decomposition temperature of the

hybrid perovskite materials is very low, the growth of single crystal hybrid perovskite materials are predominately solution based. $CH_3NH_3PbI_3$ single crystals produced by Huang et. al were of size up to 10 mm via a supersaturated precursor solution using a top-seeded solution-growth [29]. It is reported that the carrier diffusion length measured in organometal trihalide perovskite is strongly dependent on material morphology. $CH_3NH_3PbI_3$ single crystals reported by Grancini et al. are spatially in homogeneous, especially at their edge surfaces exhibiting a larger band gap and shorter carrier recombination dynamics with respect to the center due to the nature of the structure, which is attributed to surface reconstruction at the crystal edges [64].

Noel et al. reported the first demonstration of an efficient, completely lead-free perovskite solar cell using the Sn-based perovskite, $CH_3NH_3SnI_3$ as the absorber layer from which it is evident that photovoltaic performance is not limited to lead-based perovskites [58]. Though these devices yield efficiency >6% stability if the material is still a challenge [65]. Diffusion length reported was approximately 30 nm, however, the diffusion length is limited by recombination with self-doping carriers. If the stability of the lead-free material is addressed then usage of these materials in device applications will be overwhelming. J. Su et al. reported the large $CH_3NH_3PbX_3$ (I, Br) single crystals sized up to 1 cm which are grown using hydrohalic acid solution and characterized for lattice parameters (5.9345 Å with the cubic structure) [66].

The metal-organic perovskite films were fabricated by spin coating on each substrate the precursor solution consisting of CH_3NH_3I and the $PbCl_2$ dissolved in solvent. It is reported that the longer annealing times lead to decomposition of the films whereas the reduced annealing time helps a faster kinetic for the crystallization of the perovskites on ZnO substrates which is reported mainly due to different surface chemistry [59, 67]. It is also reported that the crystallization time and thin film structure are strongly influenced by the chemical nature and porosity of the substrate particularly crystals of nanometer size porous scaffold give a shorter-living and blue-shifted emission with respect to the crystals which are grown without any constraints.

4. Conclusion

Perovskite solar cells with OMH perovskite material, enhances the kinetics of the solar cell device in terms of light sensitivity, absorbance, ambipolar electron-hole transportation. OMH perovskite materials also exhibit good electrical properties such as a direct, low bandgap with superior carrier mobility, significant ferroelectric, and dielectric properties. Though PSC with perovskite in the film form are attractive with their higher performance, they degrade at faster rate, suffer immensely from a high density of traps and grain boundaries, which markedly limit the potential performance in devices. PSC with single crystalline perovskite materials have great potential to boost photovoltaic device power conversion efficiency to 25%. Organometal trihalide perovskites or $MAPbX_3$ structured single crystals are very promising in the PSC with the best set of reported properties so far to be used as the commercial devices.

Acknowledgements

The authors acknowledge AAMU-DHS-BS Award #2010-ST-062-000034, AAMU-NSF-REU award # PHY -1559870, and XULA CUR grant.

References

[1] G. Hodes, Perovskite-based solar cells, Science. 342 (2013) 317–8. doi: 10.1126/science.1245473.

[2] M. A. Green, A. Ho-Baillie, H. J. Snaith, The emergence of perovskite solar cells, Nat. Photonics. 8 (2014) 506–514. doi: 10.1038/nphoton.2014.134.

[3] P. Gao, M. Grätzel, M. K. Nazeeruddin, Organohalide lead perovskites for photovoltaic applications, Energy Environ. Sci. 7 (2014) 2448–2463. doi: 10.1039/c4ee00942h.

[4] H. J. Snaith, A. Abate, J. M. Ball, G. E. Eperon, T. Leijtens, N. K. Noel, S. D. Stranks, J. T.-W. Wang, K. Wojciechowski, W. Zhang, Anomalous Hysteresis in Perovskite Solar Cells, J. Phys. Chem. Lett. 5 (2014) 1511–1515. doi: 10.1021/jz500113x.

[5] N.-G. Park, Perovskite solar cells: an emerging photovoltaic technology, Mater. Today. 18 (2015) 65–72. doi: 10.1016/j.mattod.2014.07.007.

[6] A. K. Chilvery, A. K. Batra, B. Yang, K. Xiao, P. Guggilla, M. D. Aggarwal, R. Surabhi, R. B. Lal, J.. Currie, B. G. Penn, Perovskites: transforming photovoltaics, a mini-review, J. Photonics Energy. 5 (2015) 57402.

[7] A. G. Martin, E. Keith, H. Yoshihiro, W. Wilhelm, D. D. Ewan, Solar cell efficiency tables (version 47), Prog. Photovolt Res. Appl. 24 (2016) 3–11. doi: 10.1002/pip.

[8] NREL Efficiency Chart, 2016. http://www.nrel.gov/ncpv/images/efficiency_chart.jpg.

[9] W. S. Yang, J. H. Noh, N. J. Jeon, Y. C. Kim, S. Ryu, J. Seo, S. Il Seok, High-performance photovoltaic perovskite layers fabricated through intramolecular exchange, Science. 348 (2015) 1234–1237.

[10] A. Marchioro, J. Teuscher, D. Friedrich, M. Kunst, R. van de Krol, T. Moehl, M. Grätzel, J.-E. Moser, Unravelling the mechanism of photoinduced charge transfer processes in lead iodide perovskite solar cells, Nat. Photonics. 8 (2014) 250–255. doi: 10.1038/nphoton.2013.374.

[11] G. Giorgi, J. Fujisawa, H. Segawa, K. Yamashita, Small Photocarrier Effective Masses Featuring Ambipolar Transport in Methylammonium Lead Iodide Perovskite: A Density Functional Analysis, J. Phys. Chem. Lett. 4 (2013) 4213–4216.

[12] A. Kojima, K. Teshima, Y. Shirai, T. Miyasaka, Organometal halide perovskites as visible-light sensitizers for photovoltaic cells, J. Am. Chem. Soc. 131 (2009) 6050–6051. doi: 10.1021/ja809598r.

[13] D. Liu, T. L. Kelly, Perovskite solar cells with a planar heterojunction structure prepared using room-temperature solution processing techniques, Nat. Photonics. 8 (2013) 133–138. doi: 10.1038/nphoton.2013.342.

[14] C. Kagan, D. Mitzi, C. Dimitrakopoulos, Organic-inorganic hybrid materials as semiconducting channels in thin-film field-effect transistors, Science. 286 (1999) 945–947. http://www.ncbi.nlm.nih.gov/pubmed/10542146.

[15] S. A. Bretschneider, J. Weickert, J. a. Dorman, L. Schmidt-Mende, Physical and electrical characteristics of lead halide perovskites for solar cell applications, APL Mater. 2 (2014) 40701. doi: 10.1063/1.4871795.

[16] E. J. Juarez-Perez, R. S. Sanchez, L. Badia, G. Garcia-Belmonte, Y. S. Kang, I. Mora-Sero, J. Bisquert, Photoinduced Giant Dielectric Constant in Lead Halide Perovskite Solar Cells, J. Phys. Chem. Lett. 5 (2014) 2390–2394. doi: 10.1021/jz5011169.

[17] Y. Fu, H. Zhu, A. W. Schrader, D. Liang, Q. Ding, P. Joshi, L. Hwang, X. Y. Zhu, S. Jin, Nanowire Lasers of Formamidinium Lead Halide Perovskites and Their Stabilized Alloys with Improved Stability, Nano Lett. 16 (2016) 1000–1008. doi: 10.1021/acs.nanolett.5b04053.

[18] M. I. Saidaminov, A. L. Abdelhady, B. Murali, E. Alarousu, V. M. Burlakov, W. Peng, I. Dursun, L. Wang, Y. He, G. Maculan, A. Goriely, T. Wu, O. F. Mohammed, O. M. Bakr, High-quality bulk hybrid perovskite single crystals within minutes by inverse temperature crystallization, Nat. Commun. 6 (2015) 7586. doi: 10.1038/ncomms8586.

[19] C. C. Stoumpos, C. D. Malliakas, M. G. Kanatzidis, Semiconducting tin and lead iodide perovskites with organic cations: phase transitions, high mobilities, and near-infrared photoluminescent properties, Inorg. Chem. 52 (2013) 9019–9038.

[20] A. D. Sheikh, A. Bera, A. Haque, R. B. Rakhi, S. Del, H. N. Alshareef, T. Wu, Atmospheric effects on the photovoltaic performance of hybrid perovskite solar cells, Sol. Energy Mater. Sol. Cells. 137 (2015) 6–14. doi: 10.1016/j.solmat.2015.01.023.

[21] M. Meister, Charge Generation and Recombination in Hybrid Organic / Inorganic Solar Cells, Johannes Gutenberg-University Mainz, 2013.

[22] H.-S. Kim, S. H. Im, N.-G. Park, Organolead Halide Perovskite: New Horizons in Solar Cell Research, J. Phys. Chem. C. 118 (2014) 5615–5625. doi: 10.1021/jp409025w.

[23] N. Park, Organometal Perovskite Light Absorbers Toward a 20% Efficiency Low-Cost Solid-State Mesoscopic Solar Cell, J. Phys. Chem. Lett. 4 (2013) 2423–2429.

[24] J. H. Noh, S. H. Im, J. H. Heo, T. N. Mandal, S. Il Seok, Chemical management for colorful, efficient, and stable inorganic-organic hybrid nanostructured solar cells, Nano Lett. 13 (2013) 1764–1769. doi: 10.1021/nl400349b.

[25] O. Malinkiewicz, A. Yella, Y. H. Lee, G. M. Espallargas, M. Graetzel, M. K. Nazeeruddin, H. J. Bolink, Perovskite solar cells employing organic charge-transport layers, Nat. Photonics. 8 (2013) 128–132. doi: 10.1038/nphoton.2013.341.

[26] H. S. Kim, N.-G. Park, Parameters Affecting I-V Hysteresis of $CH_3NH_3PbI_3$ Perovskite Solar Cells: Effects of Perovskite Crystal Size and Mesoporous TiO_2 Layer, J. Phys. Chem. Lett. 5 (2014) 2927–2934. doi: 10.1021/jz501392m.

[27] R. S. Sanchez, V. Gonzalez-Pedro, J.-W. Lee, N.-G. Park, Y. S. Kang, I. Mora-Sero, J. Bisquert, Slow Dynamic Processes in Lead Halide Perovskite Solar Cells. Characteristic Times and Hysteresis, J. Phys. Chem. Lett. 5 (2014) 2357–2363. doi: 10.1021/jz5011187.

[28] X. W. Zhou, F. P. Doty, P. Yang, Atomistic Models for Scintillatory Discovery, in: F. P. Doty, H. B. Barber, H. Roehrig, R. C. Schirato (Eds.), Penetrating Radiat. Syst. Appl. XI, 2010: p. 78060E1-78060E6. doi: 10.1117/12.864152.

[29] J. Huang, Y. Shao, Q. Dong, Organometal Trihalide Perovskite Single Crystals: A Next Wave of Materials for 25% Efficiency Photovoltaics and Applications Beyond?, J. Phys. Chem. Lett. 6 (2015) 3218–3227. doi: 10.1021/acs.jpclett.5b01419.

[30] V. M. Goldschmidt, Geochemisce Verterlungsgesetze der Elemente, Oslo, 1927.

[31] M. Johnsson, P. Lemmens, Crystallography and Chemistry of Perovskites, in: John Wiley Sons, Ltd, New York, 2007: p. 11. doi: 10.1002/9780470022184.hmm411.

[32] S. B. Hendricks, Z. Kristallogr, The Crystal Structure of Perovskites, 67 (1928) 106.

[33] E. W. Hughes, W. N. Lipscomb, The Crystal Structure of Methylammonium Chloride, J. Am. Chem. Soc. 68 (1946) 1970–1975.

[34] E. J. Gabe, The crystal structure of methylammonium bromide, Acta Crystallogr. 14 (1961) 1296–1296. doi: 10.1107/S0365110X6100382X.

[35] J. Fan, B. Jia, M. Gu, Perovskite-based low-cost and high-efficiency hybrid halide solar cells, Photonics Res. 2 (2014) 111. doi: 10.1364/PRJ.2.000111.

[36] D. B. Mitzi, M. T. Prikas, K. Chondroudis, Thin Film Deposition of Organic - Inorganic Hybrid Materials Using a Single Source Thermal Ablation Technique, Chem. Mater. 11 (1999) 542–544.

[37] D. B. Mitzi, Templating and structural engineering in organic–inorganic perovskites, Dalt. Trans. 1 (2001) 1–12. doi: 10.1039/b007070j.

[38] D. B. Mitzi, K. Chondroudis, C. R. Kagan, Organic-Inorganic Electronics, IBM J. Res. Dev. 45 (2001) 29–45.

[39] D. B. Mitzi, Synthesis, Structure, and Properties of Organic-Inorganic Perovskites and Related Materials, John Wiley & Sons, West Sissex, England, New York, 1999.

[40] J. L. Knutson, J. D. Martin, D. B. Mitzi, Tuning the band gap in hybrid tin iodide perovskite semiconductors using structural templating, Inorg. Chem. 44 (2005) 4699–705. doi: 10.1021/ic050244q.

[41] N. Espinosa, L. Serrano-luján, A. Urbina, F. C. Krebs, Solution and vapour deposited lead perovskite solar cells : Ecotoxicity from a life cycle assessment perspective, Sol. Energy Mater. Sol. Cells. 137 (2015) 303–310. doi: 10.1016/j.solmat.2015.02.013.

[42] G. Kieslich, S. Sun, T. Cheetham, An Extended Tolerance Factor Approach for Organic-Inorganic Perovskites, Chem. Sci. 6 (2015) 3430–3433. doi: 10.1039/C5SC00961H.

[43] A. Chilvery, S. Das, P. Guggilla, C. Brantley, A. Sunda-meya, A perspective on the recent progress in solution- processed methods for highly efficient perovskite solar cells, Sci. Technol. Adv. Mater. 17 (2016) 1–9. doi: 10.1080/14686996.2016.1226120.

[44] M. A. Loi, J. C. Hummelen, Hybrid solar cells: Perovskites under the Sun, Nat. Mater. 12 (2013) 1087–9. doi: 10.1038/nmat3815.

[45] Y. Dang, Y. Liu, Y. Sun, D. Yuan, X. Liu, W. Lu, G. Liu, H. Xia, X. Tao, Bulk Crystal Growth of Hybrid Perovskite Material CH3NH3PbI3. CrystEngComm 2015, 17, 665−670. (49) Weller, M. T.; Weber, O. J.; Henry, P. F.; Di, Cryst. Eng. Commun. 17 (2015) 665–670.

[46] T. C. Weller, M. T.; Weber, O. J.; Henry, P. F.; Di Pumpo, A. M.; Hansen, Complete Structure and Cation Orientation in the Perovskite Photovoltaic Methylammonium Lead Iodide Between 100 and 352 K, Chem. Commun. 51 (2015) 4180–4183.

[47] C. Quarti, E. Mosconi, F. De Angelis, Structural and Electronic Properties of Organo-Halide Hybrid Perovskites from Ab Initio Molecular Dynamics, Phys. Chem. Chem. Phys. 17 (2015) 9394−9409.

[48] M. A. Carignano, A. Kachmar, J. Hutter, Thermal Effects on CH3NH3PbI3 Perovskite from Ab Initio Molecular Dynamics Simulations, J. Phys. Chem. 119 (2015) 8991−8997.

[49] J. M. Frost, K. T. Butler, A. Walsh, Molecular ferroelectric contributions to anomalous hysteresis in hybrid perovskite solar cells, APL Mater. 2 (2014) 81506. doi: 10.1063/1.4890246.

[50] F. Zheng, D. Saldana-Greco, S. Liu, A. M. Rappe, Material Innovation in Advancing Organometal Halide Perovskite Functionality, J. Phys. Chem. Lett. 6 (2015) 4862–4872. doi: 10.1021/acs.jpclett.5b01830.

[51] Y. Yang, Y. Yan, M. Yang, S. Choi, K. Zhu, J. M. Luther, M. C. Beard, Low surface recombination velocity in solution-grown CH3NH3PbBr3 perovskite single crystal, Nat Commun. 6 (2015) 7961. doi: 10.1038/ncomms8961.

[52] F. Yongping, M. Fei, R. Matthew B, M. Blaise J, Thompson Shearer, M. Dewei, H. Robert J, W. John, J. Song, Solution Growth of Single Crystal Methylammonium Lead Halide Perovskite Nanostructures for Optoelectronic and Photovoltaic Applications, J. Am. Chem. Soc. 137 (2015) 5810–5818.

[53] M. De Bastiani, V. D'Innocenzo, S. D. Stranks, H. J. Snaith, A. Petrozza, Role of the crystallization substrate on the photoluminescence properties of organo-lead mixed halides perovskites, APL Mater. 2 (2014) 81509. doi: 10.1063/1.4889845.

[54] W. Nie, H. Tsai, R. Asadpour, J. Blancon, A. J. Neukirch, G. Gupta, J. J. Crochet, M. Chhowalla, S. Tretiak, M. A. Alam, H. Wang, A. D. Mohite, High-efficiency solution-processed perovskite solar cells with millimeter-scale grains, Science (80-.). 347 (2015) 522–525.

[55] D. Shi, V. Adinolfi, R. Comin, M. Yuan, E. Alarousu, A. Buin, Y. Chen, S. Hoogland, A. Rothenberger, K. Katsiev, Y. Losovyj, X. Zhang, P. A. Dowben, O. F. Mohammed, E. H. Sargent, O. M. Bakr, Low trap-state density and long carrier diffusion in organolead trihalide perovskite single crystals, Science. 347 (2015) 519–522.

[56] Q. Dong, Y. Fang, Y. Shao, P. Mulligan, J. Qiu, L. Cao, J. Huang, Electron-hole diffusion lengths > 175 um in solution-grown CH 3 NH 3 PbI 3 single crystals, Science. 347 (2015) 967–970.

[57] A. Pisoni, J. Jaćimović, O. S. Barišić, M. Spina, R. Gaál, L. Forró, E. Horváth, Ultra-Low Thermal Conductivity in Organic–Inorganic Hybrid Perovskite CH 3 NH 3 PbI 3, J. Phys. Chem. Lett. (2014) 2488–2492. doi: 10.1021/jz5012109.

[58] N. K. Noel, S. D. Stranks, A. Abate, C. Wehrenfennig, S. Guarnera, A.-A. Haghighirad, A. Sadhanala, G. E. Eperon, S. K. Pathak, M. B. Johnston, A. Petrozza, L. M. Herz, H. J. Snaith, Lead-Free Organic-Inorganic Tin Halide Perovskites for Photovoltaic Applications, Energy Environ. Sci. 7 (2014) 3061–3068. doi: 10.1039/C4EE01076K.

[59] G. Maculan, A. D. Sheikh, A. L. Abdelhady, M. I. Saidaminov, M. A. Haque, B. Murali, E. Alarousu, O. F. Mohammed, T. Wu, O. M. Bakr, CH3NH3PbCl3 Single Crystals: Inverse Temperature Crystallization and Visible-Blind UV-Photodetector, J. Phys. Chem. Lett. 6 (2015) 3781–3786. doi: 10.1021/acs.jpclett.5b01666.

[60] F. Hao, C. C. Stoumpos, D. H. Cao, R. P. H. Chang, M. G. Kanatzidis, Lead-free solid-state organic–inorganic halide perovskite solar cells, Nat. Photonics. 8 (2014) 489–494. doi: 10.1038/nphoton.2014.82.

[61] S. Brittman, G. Erik C, Measuring n and k at the Microscale in Single Crystals of CH3NH3PbBr3 Perovskite, J. Phys. Chem. C. 120 (2016) 616–620.

[62] W. Tang, J. Hai, Y. Dai, Z. Huang, B. Lu, F. Yuan, J. Tang, F. Zhang, Recent development of conjugated oligomers for high-efficiency bulk-heterojunction solar cells, Sol. Energy Mater. Sol. Cells. 94 (2010) 1963–1979. doi: 10.1016/j.solmat.2010.07.003.

[63] M. I. Saidaminov, A. L. Abdelhady, G. Maculan, O. M. Bakr, Retrograde solubility of formamidinium and methylammonium lead halide perovskites enabling rapid single crystal growth, Chem. Commun. 51 (2015) 17658–17661. doi: 10.1039/C5CC06916E.

[64] G. Grancini, V. D'Innocenzo, E. R. Dohner, N. Martino, A. R. Srimath Kandada, E. Mosconi, F. De Angelis, H. I. Karunadasa, E. T. Hoke, A. Petrozza, CH3NH3PbI3 Perovskite Single Crystals: Surface Photophysics and its Interaction with the Environment, Chem. Sci. 6 (2015) 7305–7310. doi: 10.1039/C5SC02542G.

[65] M. H. Kumar, S. Dharani, W. L. Leong, P. P. Boix, R. R. Prabhakar, T. Baikie, C. Shi, H. Ding, R. Ramesh, M. Asta, M. Graetzel, S. G. Mhaisalkar, N. Mathews, Lead-Free Halide Perovskite Solar Cells with High Photocurrents Realized Through Vacancy Modulation, Adv. Mater. 26 (2014) 7122–+. doi: 10.1002/adma.201401991.

[66] J. Su, D. P. Chen, C. T. Lin, Growth of large CH3NH3PbX3 (X=I, Br) single crystals in solution, J. Cryst. Growth. 422 (2015) 75–79. doi: 10.1016/j.jcrysgro.2015.04.029.

[67] K. Park, J. W. Lee, J. D. Kim, N. S. Han, D. M. Jang, S. Jeong, J. Park, J. K. Song, Light-Matter Interactions in Cesium Lead Halide Perovskite Nanowire Lasers, J. Phys. Chem. Lett. (2016) acs.jpclett.6b01821. doi: 10.1021/acs.jpclett.6b01821.